Estimating Pentose Phosphate Pathway Activity From the Analysis of Hepatic Glycogen ^{13}C-Isotopomers Derived From [U-^{13}C]Fructose and [U-^{13}C]Glucose

Getachew D. Belew[#], Giada Di Nunzio[#], Ludgero Tavares, Joao G. Silva, Alejandra N. Torres, and John G. Jones*

Center for Neurosciences and Cell Biology, University of Coimbra, Portugal

***Address for Correspondence:**

John G. Jones,

Center for Neurosciences and Cell Biology

UC-Biotech, Biocant Park

3060-197, Cantanhede, Portugal

[#]Joint first authors

email: john.griffith.jones@gmail.com

Word Count: 2346

Abstract (244 words)

Purpose: The pentose phosphate pathway (PPP) is an important component of hepatic intermediary metabolism. Jin et al. developed an elegant ^{13}C-NMR method for measuring hepatic PPP flux by quantifying the distribution of glucose ^{13}C-isotopomers formed from [U-^{13}C]glycerol. We demonstrate that this approach can be extended to exogenous [U-^{13}C]fructose and [U-^{13}C]glucose precursors by ^{13}C-NMR analysis of glycogen.

Methods: Twelve male C57BL/6 mice fed standard chow were provided a 55/45 mixture of fructose and glucose at 30% w/v in the drinking water for 18 weeks. On the evening before sacrifice, the fructose component was enriched with 20% [U-^{13}C]fructose for 6 mice while the glucose component was enriched with 20% [U-^{13}C]glucose for the remaining 6 mice. Mice were allowed to feed and drink naturally overnight and then euthanized. Livers were freeze-clamped and glycogen was extracted and derivatized for ^{13}C NMR spectroscopy. Flux of each sugar into the PPP relative to its incorporation into glycogen was quantified from selected ^{13}C glycogen isotopomer ratios.

Results: Both [U-^{13}C]fructose and [U-^{13}C]glucose precursors yielded glycogen ^{13}C-isotopomer distributions that were characteristic of PPP activity. The fraction of [U-^{13}C]glucose utilized by the PPP relative to its conversion to glycogen via the direct pathway was 14±1% while that from [U-^{13}C]fructose relative to its conversion to glycogen via the indirect pathway was significantly lower (10±1%, p=0.00032).

Conclusions: Hepatic PPP fluxes from both [U-^{13}C]glucose and [U-^{13}C]fructose precursors were assessed by ^{13}C NMR analysis of glycogen ^{13}C-isotopomers. Glucose-6-phosphate generated via glucokinase and the direct pathway is preferentially utilized by the PPP.

Keywords: NADPH, indirect pathway, NMR, glucokinase,

Introduction:

The pentose phosphate pathway (PPP) plays a critical role in intermediary metabolism by providing NADPH for both biosynthetic activities and regeneration of reduced glutathione as well as ribose-5-phosphate for nucleotide biosynthesis. In the liver, there is high interest in the role of the PPP in the pathogenesis of diseases such as non-alcoholic fatty liver disease (NAFLD) – where PPP activity may be linked to elevated rates of *de novo* lipogenesis (1) - and hepatocellular carcinoma, where among other things, *de novo* synthesis of nucleotides is upregulated (2). Recently, a stable-isotope tracer method for quantifying hepatic PPP activity by analysis of plasma glucose ^{13}C-isotopomers generated from [U-^{13}C]glycerol was reported (1,3,4). The ^{13}C-label reaches glucose-6-P via gluconeogenesis and the glucose ^{13}C-isotopomer distribution reports the proportion of ^{13}C-enriched glucose-6-P that was directly converted to glucose, *versus* the fraction that had cycled through the PPP beforehand. Previously, in most cases, PPP fluxes had been evaluated with a labeled glucose precursor by analyzing the label distribution in a downstream glycolytic product such as lactate (5-7). In the liver, glucose-6-P enrichment from both glucose and gluconeogenic ^{13}C-tracers is transferred to glycogen via the so-called direct and indirect pathways (8). Therefore, we applied the hexose ^{13}C-isotopomer analysis developed by Jin et al. (1,3,4) to liver glycogen to determine the extent of PPP metabolism of exogenous [U-^{13}C]glucose and [U-^{13}C]fructose destined for hepatic glycogen synthesis.

Methods:

Materials: [U-^{13}C]fructose at 99% enrichment was obtained from Omicron Biochemicals Inc., IN, USA and [U-^{13}C]glucose at 99% enrichment was manufactured by Cambridge Isotopes Limited, Cambridge, MA, USA and purchased though Tracertec, Madrid, Spain.

Animal Studies: Animal studies were approved by the University of Coimbra Ethics Committee on Animal Studies (ORBEA) and the Portuguese National Authority for Animal Health (DGAV),

approval code 0421/000/000/2013. Adult male C57BL/6 mice were obtained from Charles River Labs, Barcelona, Spain, and housed at the UC Biotech Bioterium. They were maintained in a well-ventilated environment, and a 12h light/12h dark cycle. Upon delivery to the Bioterium, mice were provided a two week interval for acclimation, with free access to water and standard chow. After this period, the drinking water was supplemented with a 55/45 mixture of fructose and glucose. This mixture was present at a concentration of 30% w/v and was provided for a period of 18 weeks. On the ultimate evening, the fructose/glucose mixture was replaced with a mixture where the fructose was enriched to 20% with [U-^{13}C]fructose for six of the mice, with the remaining six provided with a mixture where the glucose was enriched to 20% with [U-^{13}C]glucose. As part of a separate study on triglyceride and glycogen synthesis sources, the mice also received 99.8% deuterated water ($^{2}H_2O$) with 0.9% NaCl as an intraperitoneal loading dose (4 g/100 g body weight) at the start of the evening while the drinking water was enriched to 5% with $^{2}H_2O$ throughout the night. At the end of this dark cycle, mice were deeply anesthetized with ketamine/xylazine and sacrificed by cardiac puncture. Livers were freeze-clamped and stored at -80ºC until further analysis.

Glycogen extraction and monoacetone glucose synthesis: Samples were prepared as described previously by Rito at al. (9) Briefly, glycogen was extracted from frozen liver powder after basic digestion with 30% KOH (2 ml/g of liver) at 70ºC for 1 hour. The mixture was treated with 6% Na_2SO_4 (1 ml/g of liver) and glycogen precipitated with ethanol (7 ml/g of liver). After centrifugation, the pellet was dried and resuspended in acetate buffer (0.05 M, pH = 4.5). Aqueous solution containing 20 U of amyloglucosidase from *Aspergillus niger* (Glucose-free preparation, Sigma-Aldrich, Germany) was added and incubated overnight at 55ºC. The supernatant was lyophilized and mixed with 5 ml ^{2}H-enriched acetone prepared as described (10) and 4% sulphuric acid enriched to 2% with $^{2}H_2SO_4$ (v/v). The mixture was stirred overnight at room temperature. The reaction was quenched with water (5 ml, enriched to 2% with $^{2}H_2O$), adjusted to pH=2.0 and

incubated at 40ºC for 5 hours. The solution pH was adjusted to 8 with $NaHCO_3$ and the samples evaporated to dryness. Monoacetone glucose (MAG) in the residue was extracted with boiling ethyl acetate. Ethyl acetate was evaporated, the residue dissolved in H_2O and purified by solid phase Discovery® DSC-18 3 mL/500 mg disposable columns (Sigma-Aldrich) as previously described (9). MAG samples were dissolved in 0.2 ml 99.9% ^2H_2O for ^{13}C NMR analysis.

NMR analysis: Proton-decoupled ^{13}C NMR spectra were obtained with a Varian VNMRS 600 MHz NMR (Agilent) spectrometer equipped with a 3-mm broadband probe. ^{13}C NMR spectra were acquired at 25 ºC using a 60º pulse, 30.5 kHz spectral width and 4.1 s of recycling time (4.0 s of acquisition time and 0.1 s pulse delay). The number of acquisitions ranged from 2,000 to 12,000. The spectra were processed with 0.2 Hz line-broadening before Fourier transformation. Spectra were analyzed using NUTS PC-based NMR spectral analysis software (Acorn NMR Inc., USA).

Quantification of PPP fluxes: PPP fluxes were quantified from the analysis of glycogen carbon 2 and carbon 5 ^{13}C-isotopomer multiplets based on the method of Jin et al. for [U-^{13}C]glycerol (3,4). Translating this method to [U-^{13}C]fructose is straightforward since this sugar is metabolized to the same triose-P intermediates as glycerol. In the case of [U-^{13}C]glucose, although the initial pentose phosphate intermediates are uniformly enriched following the oxidative removal of carbon 1, the subsequent transaldolase/transketolase exchange pathways generate [1,2-$^{13}C_2$]fructose-6-P that is stoichiometric with the oxidative PPP step (Figure 1). Thus, quantification of the resulting [1,2-$^{13}C_2$]glycogen isotopomer from the ^{13}C NMR doublet 12 signal component ($D12_{PPP}$) with correction for contributions from non-PPP activity (1,3,4), can yield fractional PPP rates relative to the conversion of [U-^{13}C]glucose to glycogen.

$$D12_{PPP} = D12_{total} - D12_{KC} \quad (1)$$

Where $D12_{total}$ is the observed doublet fraction relative to all other carbon 2 signals and $D12_{KC}$ is the doublet contribution from Krebs cycle sources. $D12_{KC}$ was estimated as follows (1,3,4):

$$D12_{KC} = D23 \times D56/D45 \quad (2)$$

Where D23 is the area of the 2,3-^{13}C doublet relative to the total carbon 2 signal and D56 and D45 are the areas of the 5,6-^{13}C and 4,5-^{13}C doublet signals relative to the total carbon 5 signal, respectively.

The ^{13}C-fractional enrichment of the $D12_{PPP}$ component was estimated as follows:

$$D12_{PPP} \text{ fractional } ^{13}\text{C-enrichment (\%)} = D12_{PPP} \text{ signal area/carbon 2 singlet area} \times 1.11 \quad (3)$$

The fraction of [U-^{13}C]glucose utilized by the PPP relative to that entering the direct pathway was estimated from the ratios of glycogen $D12_{PPP}$ and [U-^{13}C]glycogen fractional ^{13}C-enrichments as follows:

$$[\text{U-}^{13}\text{C}]\text{glucose PPP fraction} = 100 \times D12_{PPP} / [\text{U-}^{13}\text{C}]\text{glycogen fractional } ^{13}\text{C-enrichment} \quad (4)$$

Where the [U-^{13}C]glucose fractional ^{13}C-enrichment was calculated from the MAG carbon 1 multiplet as previously described (9,11).

The fraction of [U-^{13}C]fructose utilized by the PPP relative to that entering glycogen via the indirect pathway was estimated from the ratios of glycogen $D12_{PPP}$ and [4,5,6-^{13}C]glycogen fractional ^{13}C-enrichments as follows:

[U-^{13}C]fructose PPP fraction = $D12_{PPP}$/[4,5,6-^{13}C]glycogen fractional ^{13}C-enrichment (5)

The [4,5,6-^{13}C]glycogen fractional ^{13}C-enrichment was measured from the ratio of the carbon 5 quartet and singlet as follows:

[4,5,6-^{13}C]glycogen fractional ^{13}C-enrichment (%) = carbon 5 quartet/singlet × 1.11 (6)

Statistics: All results are presented as means ± standard error and comparisons were made by an unpaired t-test (two tailed) performed using Microsoft Excel. Statistical significance was defined by p values of < 0.05.

Results:

The ^{13}C NMR signals of carbons 2 and 5 of MAG derived from hepatic glycogen of a mouse provided with [U-^{13}C]glucose are shown in Figure 2. The multiplet (M) component of the carbon 2 signal represents a mixture of [U-^{13}C]glucose and [1,2,3-$^{13}C_3$]glucose isotopomers while the M component of the carbon 5 resonance represents a mixture of [U-^{13}C]glucose and [4,5,6-$^{13}C_3$]glucose isotopomers. Its complex structure reflects the presence of long-range ^{13}C-^{13}C couplings within the [U-^{13}C]glucose moiety between carbons 5 and 1, carbons 5 and 2, and carbons 5 and 3 (11). Likewise, the M component of carbon 2 features long-range ^{13}C-^{13}C couplings between carbon 2 and 4, and carbons 2 and 5 (11). The low intensities of the D45 and D56 components relative to M reflect the minor proportion of ^{13}C-isotopomers that were formed via the indirect pathway and Krebs cycle relative to direct pathway conversion of [U-^{13}C]glucose to glycogen. In the carbon 2 resonance, the D23 contribution, which also represents ^{13}C-Krebs cycle isotopomers, was correspondingly low in relation to the M signals. In comparison, the D12 signal was substantially stronger, indicative of PPP metabolism of the [U-^{13}C]glucose precursor.

The carbon 2 and 5 resonances of MAG obtained from a mouse provided with a mixture of unlabeled glucose and [U-^{13}C]fructose are also shown in Figure 2. Qualitatively, the main difference between these resonances and those derived from [U-^{13}C]glucose is the presence of well-resolved quartet structures for both carbons 2 and 5 reflecting the presence of discrete [1,2,3-$^{13}C_3$]- and [4,5,6-$^{13}C_3$]glycogen isotopomers. This resembles the glucose carbon 2 and carbon 5 multiplet structures observed in rats that were administered with [U-^{13}C]glycerol (1,3,4).

Quantitatively, direct pathway metabolism of [U-^{13}C]glucose and indirect pathway metabolism of [U-^{13}C]fructose via triose-P yielded similar enrichments of [U-^{13}C]glycogen and [4,5,6-$^{13}C_3$]glycogen isotopomers (see Table 1). Considering the abundances of these primary isotopomers plus pentose phosphate pathway contributions ([1,2-$^{13}C_2$]glycogen$_{PPP}$), exogenous fructose and glucose contributed almost equally to hepatic glycogen synthesis with 15 ± 1% derived from fructose and 14 ± 2% from glucose. For the [U-^{13}C]fructose experiments, while the

proportion of ^{13}C-isotopomers derived via the Krebs cycle was small in comparison to those derived via triose-P, it was nevertheless substantially higher compared to that from the [U-^{13}C]glucose experiments (see Table 1). Thus, the ratio of [2,3-$^{13}C_2$]/[4,5,6-$^{13}C_3$]glycogen from the [U-^{13}C]fructose study is approximately 0.036 while the ratio of [2,3-$^{13}C_2$]/[U-^{13}C]glycogen from the [U-^{13}C]glucose study is only 0.008. This resulted in substantially higher Krebs cycle contributions to the observed [1,2-$^{13}C_2$]glycogen enrichment for mice administered with [U-^{13}C]fructose compared to those given [U-^{13}C]glucose. As a result, the difference between [1,2-$^{13}C_2$]glycogen$_{total}$ and [1,2-$^{13}C_2$]glycogen$_{PPP}$ abundance was more pronounced in the [U-^{13}C]fructose compared to the [U-^{13}C]glucose studies. Finally, the ^{13}C-isotopomer data revealed that a significantly larger proportion of exogenous glucose metabolized to glycogen via the direct pathway had been recruited by the PPP in comparison to that from fructose converted to glycogen via the indirect pathway (Table 1).

Discussion

In the liver, the PPP plays a critical role in the conversion of exogenous sugars to fat by providing the necessary NADPH equivalents for fatty acid biosynthesis. While glucose is the canonical substrate for the PPP, any substrate that is converted to glucose-6-P, including glycerol and lactate, can also in principle provide carbon skeletons for this pathway (4). Our study took a recently developed assay of hepatic PPP flux based on analysis of plasma glucose ^{13}C-isotopomers derived from [U-^{13}C]glycerol (1,3,4) and adapted it to read PPP flux from other substrates, including the canonical glucose substrate. By reading ^{13}C-isotopomers of hepatic glycogen instead of plasma glucose, our approach allowed PPP utilization of glucose-6-P derived from direct pathway metabolism of glucose to be specifically measured and compared to glucose-6-P derived from gluconeogenesis. The main significance of our work is the finding that glucose-6-P formed from glucose via the direct pathway was more heavily utilized by the PPP compared to glucose-6-P derived from fructose via gluconeogenesis.

The fraction of [U-^{13}C]fructose that underwent PPP utilization prior to being converted to glycogen (10%) in our study was similar to the reported fraction of [U-^{13}C]glycerol that underwent PPP utilization prior to being converted to glucose in fed rats (8%) (4). Jin et al also measured PPP recruitment of glucose-6-P that had been synthesized from [U-^{13}C]lactate and found this contribution to be less than that from [U-^{13}C]glycerol (4). The results of our study indicate that a significantly larger fraction of glucose-6-P derived via the direct pathway was recruited by the PPP compared to glucose-6-P generated by indirect pathway metabolism of fructose. Glucose-6-P derived via the direct pathway is synthesized via glucokinase while indirect pathway glucose-6-P is generated by glucose-6-phosphate isomerase. In the fed condition, glucokinase activation is highly coupled to upregulation of the main pathways of glucose disposal such as glycogen synthesis and *de novo* lipogenesis (12). This may involve the co-ordinated activation of glucokinase and glucose-6-phosphate disposal pathways by upstream effectors such as insulin, as well as intracellular co-localization of glucokinase with the enzymes of pathways involved in glucose-6-P disposal, such as glycogen synthase (13). Under essentially the same conditions as that of the present study, we demonstrated a strong coupling of *de novo* lipogenesis from exogenous glucose with PPP activity as seen by a high fractional transfer of exogenous glucose hydrogens to newly-synthesized fatty acids via the PPP (14). Others have shown that hepatic PPP activity is more closely linked with lipogenic activity than with mitigation of oxidative stress – a process that potentially competes with biosynthetic pathways for intracellular NADPH (1). To what extent the activity and/or intracellular location of glucose-6-phosphate dehydrogenase - the committing enzyme of the PPP - is co-ordinated with that of glucokinase and glycogen synthesis is unclear. Frederiks et al. reported that glucose-6-phosphate dehydrogenase in rat liver parenchymal cells was associated with the ribosomes of granular endoplasmic reticulum (15). Agius et al. concluded that the very strong control exerted by glucokinase on the conversion of glucose to glycogen suggests that active

glucokinase and glycogen synthase exist in close proximity to each other in the cell (13). Moreover, glucose-6-phosphate derived from sources other than glucokinase is utilized to a lesser extent by glycogen synthase (16). Since glycogen synthesis is also initiated in the endoplasmic reticulum (17), this raises the possibility that glucokinase, glycogen synthase and glucose-6-phosphate dehydrogenase could be in close proximity to each other thereby explaining the higher recruitment of glucokinase-derived glucose-6-P for PPP activity as well as for glycogen synthesis. Whether glucose-6-P derived from glucokinase is always highly utilized by the PPP is unclear. For example in the initial stages of refeeding, glucokinase may be active while transcription of lipogenesis pathway enzymes may be incomplete. Under these conditions, demand for NADPH formation via PPP may be temporarily low, hence the fraction of glucose-6-P consumed by the PPP might be small.

Jin et al have successfully translated their methodology into humans with the procedure involving ingestion of a few grams of [U-^{13}C]glycerol followed by blood sampling and analysis of glucose ^{13}C-isotopomers (3). While this procedure can be used for [U-^{13}C]fructose, it cannot be applied to [U-^{13}C]glucose. This is because [U-^{13}C]glucose that participated in hepatic metabolism and was returned to the blood via glucose-glucose-6-P cycling cannot be distinguished from [U-^{13}C]glucose that appeared via absorption and was not metabolized by the liver. Alternatively, hepatic UDP-glucose ^{13}C-isotopomers, which provide equivalent information to those of glycogen, can be noninvasively assayed following conversion of UDP-glucose to glucuronide and clearance into urine. This so-called “chemical biopsy” approach involves ingestion of acetaminophen or other glucuronidation agent and can be integrated with oral ^{13}C-tracer administration in human studies (18, 19).

In conclusion, we applied the hepatic PPP analysis originally developed by Jin et al. to study PPP utilization of glucose and fructose that are destined for glycogen synthesis. From the analysis of glycogen ^{13}C-isotopomers derived from [U-^{13}C]glucose, PPP recruitment of glucose-6-phosphate derived specifically from glucokinase can be evaluated. Our results suggest that this source of

glucose-6-P is preferentially utilized for PPP flux compared to glucose-6-P obtained from indirect pathway precursors such as [U-^{13}C]fructose.

Acknowledgements: This work was financed by the European Regional Development Fund (ERDF), through the Centro 2020 Regional Operational Programme under project FCT-FEDER-02/SAICT/2017/028147 and through the COMPETE 2020 - Operational Programme for Competitiveness and Internationalisation and Portuguese national funds via FCT – Fundação para a Ciência e a Tecnologia, under project UIDB/04539/2020**.** The UC-NMR facility is supported in part by FEDER – European Regional Development Fund through the COMPETE Programme and the Portuguese Foundation for Science and Technology through grants POCI-01-0145-FEDER-007440; REEQ/481/QUI/2006, RECI/QEQ-QFI/0168/2012, CENTRO-07-CT62-FEDER-002012, and Rede Nacional de Ressonância Magnética Nuclear. GDB is supported by the European Union's Horizon 2020 Research and Innovation programme under the Marie Skłodowska-Curie Grant Agreement No. 722619 (Project FOIE GRAS). GDN and ANT are supported by Marie Skłodowska-Curie Grant Agreement No. 721236 (Project TREATMENT).

References

1. Jin ES, Lee MH, Murphy RE, Malloy CR. Pentose phosphate pathway activity parallels lipogenesis but not antioxidant processes in rat liver. American Journal of Physiology-Endocrinology and Metabolism 2018;314:E543-E551.
2. Kowalik MA, Columbano A, Perra A. Emerging role of the pentose phosphate pathway in hepatocellular carcinoma. Frontiers in Oncology 2017;7.
3. Jin ES, Sherry AD, Malloy CR. An oral load of [U-^{13}C]glycerol and blood NMR analysis detect fatty acid esterification, pentose phosphate pathway, and glycerol metabolism through the tricarboxylic acid cycle in human liver. Journal of Biological Chemistry 2016;291:19031-19041.
4. Jin ES, Sherry AD, Malloy CR. Interaction between the pentose phosphate pathway and gluconeogenesis from glycerol in the liver. Journal of Biological Chemistry 2014;289: 32593–32603.
5. Lee MH, Malloy CR, Corbin IR, Li J, Jin ES. Assessing the pentose phosphate pathway using [2,3-$^{13}C_2$]glucose. NMR in Biomedicine 2019:23, e4096.
6. Delgado TC, Castro MM, Geraldes CF, Jones JG. Quantitation of erythrocyte pentose pathway flux with [2-^{13}C]Glucose and ^{1}H NMR analysis of the lactate methyl signal. Magnetic Resonance in Medicine 2004;51:1283-1286.
7. Ross BD, Kingsley PB, Ben-Yoseph O. Measurement of pentose phosphate-pathway activity in a single incubation with [1,6-$^{13}C_2$,6,6-$^{2}H_2$]glucose. Biochemical Journal 1994;302:31-38.
8. Newgard CB, Hirsch LJ, Foster DW, McGarry JD. Studies on the mechanism by which exogenous glucose is converted into liver-glycogen in the rat - a direct or an indirect pathway. Journal of Biological Chemistry 1983;258:8046-8052.

9. Rito J, Viegas I, Pardal MA, Meton I, Baanante IV, Jones JG. Disposition of a glucose load into hepatic glycogen by direct and indirect pathways in juvenile seabass and seabream. Scientific Reports 2018;8.

10. Jones JG, Barosa C, Gomes F, Mendes AC, Delgado TC, Diogo L, Garcia P, Bastos M, Barros L, Fagulha A, Baptista C, Carvalheiro M, Caldeira MM. NMR derivatives for quantification of ^{2}H and ^{13}C-enrichment of human glucuronide from metabolic tracers. Journal of Carbohydrate Chemistry 2006;25:203-217.

11. Perdigoto R, Rodrigues TB, Furtado AL, Porto A, Geraldes C, Jones JG. Integration of [U-^{13}C]glucose and $^{2}H_2O$ for quantification of hepatic glucose production and gluconeogenesis. NMR in Biomedicine 2003;16:189-198.

12. Petersen MC, Vatner, DF, Shulman GI. Regulation of hepatic glucose metabolism in health and disease. Nature Reviews Endocrinology 2017; 13: 572-587.

13. Agius J, Peak M, Newgard CB, Gomez-Foiz AM, Guinovart J. Evidence for a role of glucose-induced translocation of glucokinase in the control of hepatic glycogen synthesis. Journal of Biological Chemistry 1996; 271: 30479-30486.

14. Belew GD, Silva J, Rito J, Tavares L, Viegas I, Teixeira J, Oliveira PJ, Macedo MP, Jones JG. Transfer of glucose hydrogens via acetyl-CoA, malonyl-CoA, and NADPH to fatty acids during de novo lipogenesis. Journal of Lipid Research 2019;60:2050-2056.

15. Frederiks WM, Vreeling-Sindelárová H. Localization of glucose-6-phosphate dehydrogenase activity on ribosomes of granular endoplasmic reticulum, in peroxisomes and peripheral cytoplasm of rat liver parenchymal cells. Histochemical Journal 2001; 33:345-53.

16. Seoane J, Gomez-Foix, AM, O'Doherty RM, Gomez-Ara C, Newgard CB, Guinovart J. Glucose 6-phosphate produced by glucokinase, but not hexokinase 1, promotes the activation of hepatic glycogen synthase. Journal of Biological Chemistry 1996; 271: 23756-23760.

17. Prats C, Graham TE, Shearer J. The dynamic life of the glycogen granule. Journal of Biological Chemistry 2018; 293: 7089-7098.

18. Barosa C, Silva C, Fagulha A, Barros L, Caldeira MM, Carvalheiro M, Jones JG. Sources of hepatic glycogen synthesis following a milk-containing breakfast meal in healthy subjects. Metabolism-Clinical and Experimental 2012;61:250-254.

19. Mendes AC, Caldeira MM, Silva C, Burgess SC, Merritt ME, Gomes F, Barosa C, Delgado TC, Franco F, Monteiro P, Providencia L, Jones JG. Hepatic UDP-glucose ^{13}C isotopomers from [U-^{13}C]glucose: A simple analysis by ^{13}C NMR of urinary menthol glucuronide. Magn Res Med 2006;56:1121-1125.

Figure Legends

Figure 1: Schematic of [U-^{13}C]glucose-6-P conversion to fructose-6-P through the PPP with the carbon skeleton passing via xylulose-5-phosphate (A) or ribose-5-phosphate (B). It is assumed that there is sufficient dilution of ^{13}C by ^{12}C such that the probability of two [U-^{13}C]pentose-P precursors interacting with each other is negligible.

Figure 2: Carbon 2 and carbon 5 resonances of glycogen following derivatization to MAG from a mouse administered with [U-^{13}C]glucose (top) and a mouse administered with [U-^{13}C]fructose (bottom). The multiplet components are indicated as follows: **S** = natural-abundance singlet, **M** = multiplet representing [1,2,3-$^{13}C_3$]- plus [U-^{13}C]glycogen in carbon 2 and [4,5,6-$^{13}C_3$]- plus [U-^{13}C]glycogen in carbon 5, **D12** = doublet representing [1,2-$^{13}C_2$]glycogen$_{total}$, **D23** = doublet representing [2,3-$^{13}C_2$]glycogen, **D45** = doublet representing [4,5-$^{13}C_2$]glycogen, **D56** = doublet representing [5,6-$^{13}C_2$]glycogen, **Q** = quartet representing [1,2,3-$^{13}C_3$]glycogen in carbon 2 and [4,5,6-$^{13}C_3$]glycogen in carbon 5.

Table 1: Selected liver glycogen ^{13}C-isotopomers from mice provided with fructose/glucose mixture in their drinking water enriched with either [U-^{13}C]fructose or [U-^{13}C]fructose. The values represent means and standard errors of six mice for each condition.

Glycogen ^{13}C-isotopomers from mice provided with [U-^{13}C]glucose and unlabeled fructose					
[U-^{13}C]GLY (%)	**[1,2-$^{13}C_2$]GLY$_{TOT}$ (%)**	**[2,3-$^{13}C_2$]GLY (%)**	**D56/D45**	**[1,2-$^{13}C_2$]GLY$_{PPP}$ (%)**	**Fraction of direct pathway glucose metabolized via PPP (%)**
2.57 (0.32)	0.39 (0.04)	0.02 (0.01)	1.18 (0.02)	0.36 (0.04)	14 (1)
Glycogen ^{13}C-isotopomers from mice provided with [U-^{13}C]fructose and unlabeled glucose					
[4,5,6-$^{13}C_3$]GLY (%)	**[1,2-$^{13}C_2$]GLY$_{TOT}$ (%)**	**[2,3-$^{13}C_2$]GLY (%)**	**D56/D45**	**[1,2-$^{13}C_2$]GLY$_{PPP}$ (%)**	**Fraction of indirect pathway fructose metabolized via PPP (%)**
2.51 (0.10)	0.38 (0.03)	0.09 (0.01)	1.60 (0.10)	0.24 (0.02)	10* (1)

*p = 0.00032 compared to PPP fraction from glucose

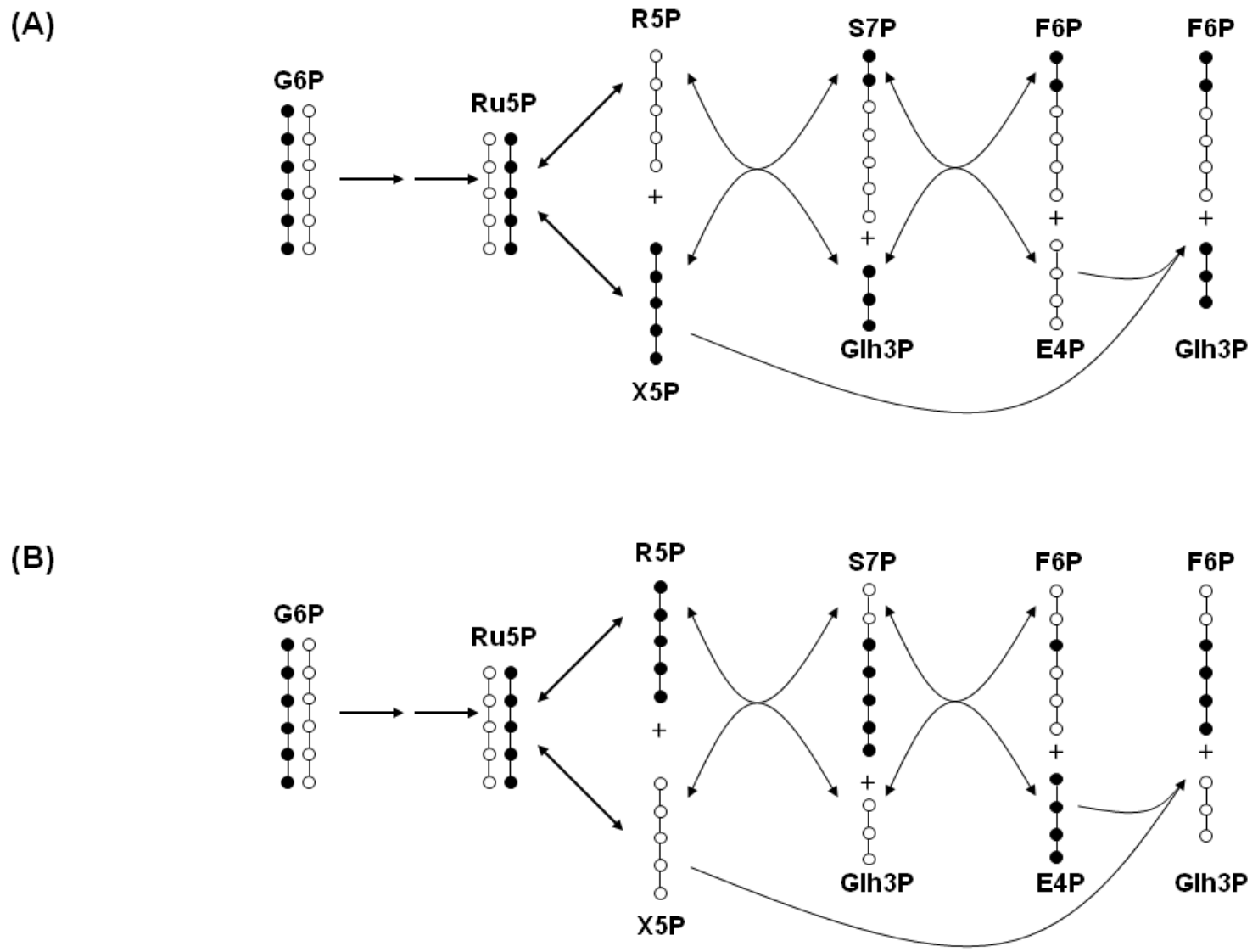
(A)
G6P
Ru5P
R5P
X5P
S7P
Glh3P
F6P
E4P
F6P
Glh3P
(B)
G6P
Ru5P
R5P
X5P
S7P
Glh3P
F6P
E4P
F6P
Glh3P

Figure 1

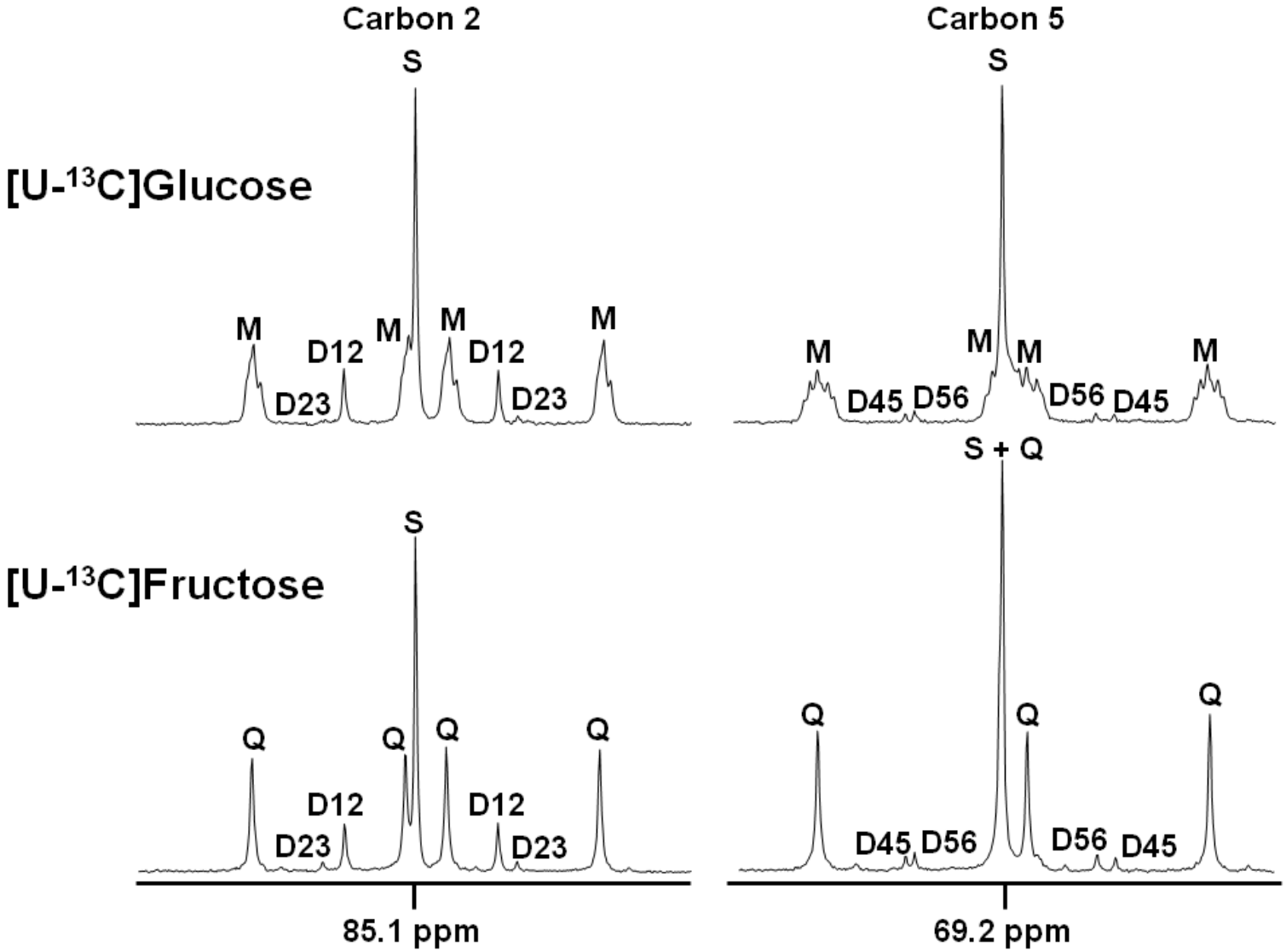
Carbon 2
Carbon 5
[U-13C]Glucose
[U-13C]Fructose
S
M
D12
D23
D45
D56
S + Q
Q
85.1 ppm
69.2 ppm

Figure 2